

In this study, the authors apply a global marine biogeochemical model to investigate the changes in the relative abundance of diatoms in response to shifts in  $\text{NH}_4\text{:DIN}$  ratio. This topic is of interest to both the modelling community and the broader research audience. Overall, the manuscript is well-written but would benefit from some structural reorganisation for readability. Additionally, several sections require further clarification and the inclusion of more supporting information.

We sincerely thank the reviewer for their positive view of our work and their thoughtful comments that have substantially improved the presentation of our work.

#### General comments

Typically, the presentation of model-data agreement (misfit) should precede the transient simulations, i.e., we should have “build confidence in the model” first. I suggest reorganising the discussion section so that the steady-state evaluation of the relationship between  $\text{NH}_4\text{:NO}_3$  and diatom abundance appears first, followed by the transient simulations. Also, the “Model experiment” section should be moved after “Statistical analyses” in the methods.

We fully acknowledge the reviewer’s suggestion and understand the motivation to rearrange the results.

In previous iterations of this manuscript, we structured the narrative to have the observed relationships first, followed by the modelling experiments. As such, our intuition was the same as the reviewer’s. However, after many iterations and constructive feedback, we were encouraged to reorder the study and place the transient modelling experiments first. The motivation to place the modelling first is to present the experiments of “model<sub>compete</sub>” as early as possible. We found that when these important results were placed at the end of the paper they were too easily lost. Meanwhile, presenting them earlier means that (1) they aren’t lost and (2) the reader is aware that this study is primarily a model study.

We do, however, very much agree with the reviewer and reviewer 1 that some clarity could be gained by presenting some aspects much earlier and a model assessment up front. As such, we have included two entirely new sections: one in the methods, and another as the first results section. Please see our answers below for the revised text and figures for these new sections.

Several statistical techniques are applied in this study. I recommend providing more background information and justification for the selected values (e.g., VIFs and spline complexity). This would help readers unfamiliar with those tools to better understand the methodological choices.

We thank the reviewer for this suggestion and have included some additional information to aid the reader in why these choices were made. Under section 2.5:

Lines 300 - 310: “We explored the environmental drivers of change in phytoplankton relative abundance data (provided by Tara Oceans) with generalized additive models (GAMs) using the *mgcv* package in R (Wood, 2006) structured as:

$$Y = \alpha + s_1(x_1) + s_2(x_2) + \dots + s_n(x_n) + \varepsilon ,$$

(6)

Where  $Y$  is the predicted response,  $\alpha$  is the intercept,  $s_n(x_n)$  represents a smooth function (specifically the  $n^{\text{th}}$  thin-plate spline) fitted to the  $n^{\text{th}}$  predictor variable  $x_n$ , and  $\varepsilon$  is the model error. Thin-plate splines are flexible and widely used as a smoothing method within GAMs that allow for non-linear relationships between predictors and response variables and do not require specificity around a functional form. They are well suited to handling ecological data where relationships are often non-linear and non-parametric. Predictor variables were mixed-layer depth (m), phosphate ( $\mu\text{M}$ ), silicate ( $\mu\text{M}$ ), dissolved iron ( $\mu\text{M}$ ), and the  $\text{NH}_4^+:\text{DIN}$  ratio. Mixed layer depth, phosphate and silicate was measured in situ at the sample locations of Tara Oceans, while dissolved iron and  $\text{NH}_4^+:\text{DIN}$  ratios were provided by the model at the same location and month of sampling, since measurements of these properties are scarce.”

Lines 331 - 333: “Before model testing, we calculated the variance inflation factors (VIFs) of independent variables to avoid multi-collinearity. All covariate VIFs were  $< 3$ , which indicates minimal multicollinearity. GAMs were computed using a low spline complexity ( $k = 3$ ) that prevented overfitting and constrained the smooth functions represent only broad-scale trends in the data.”

Although the biogeochemical model is based on a previously published version, this study applies a different nitrification configuration. The manuscript should provide at least a brief summary of how these changes affect key biogeochemical inventories (such as the relative abundance of the two phytoplankton types) and fluxes (including nitrogen fixation) to support the new model's validity.

We have provided a more extended description of the additions made to the PISCESv2 model in the methods, and provided an entirely new methods section that describes a key component of the nitrogen cycle: the nitrogen limitation parametersiation for diatoms and nanophytoplankton. We have also included a new section to the results that details a model-data assessment of N cycling in the upper ocean.

Lines 104 - 131: “The biogeochemical model is the Pelagic Interactions Scheme for Carbon and Ecosystem Studies version 2 (PISCES-v2), which is detailed and assessed in Aumont et al. (2015). This model is embedded within version 4.0 of the Nucleus for European Modelling of the Ocean (NEMO-v4.0). We chose a  $2^\circ$  nominal horizontal resolution with 31 vertical levels with thicknesses ranging from 10 meters in the upper 100 meters to 500 meters below 2000 meters. Due to the curvilinear grid, horizontal resolution increases to  $0.5^\circ$  at the equator and to near  $1^\circ$  poleward of  $50^\circ\text{N}$  and  $50^\circ\text{S}$ .

We updated the standard PISCES-v2 (Aumont et al., 2015) for the purposes of this study, specifically by adding  $\text{NO}_2^-$  as a new tracer. The PISCESv2 biogeochemical model already resolved the pools of  $\text{NH}_4^+$ ,  $\text{NO}_3^-$ , dissolved oxygen, the carbon system, dissolved iron, phosphate, two kinds of phytoplankton biomass (nanophytoplankton and diatoms), two kinds

of zooplankton biomass (micro- and meso-zooplankton), small and large pools of particulate organic matter, and dissolved organic matter (Aumont et al., 2015). While the model does not strictly represent picophytoplankton, implicit variations in the average cell size of the nanophytoplankton type affect nutrient uptake dynamics and may therefore encompass some functionality of picophytoplankton in oligotrophic systems (Aumont et al., 2015). The addition of  $\text{NO}_2^-$  necessitated breaking full nitrification ( $\text{NH}_4^+ \rightarrow \text{NO}_3^-$ ) into its two steps of ammonia ( $\text{NH}_4^+ \rightarrow \text{NO}_2^-$ ) and nitrite oxidation ( $\text{NO}_2^- \rightarrow \text{NO}_3^-$ ). Both steps were simulated implicitly by multiplying a maximum growth rate by the concentration of substrate and limitation terms representing the effect of environmental conditions to return the realized rate. For ammonia oxidation, limitations due to substrate availability, light and pH determined the realised rate. For nitrite oxidation, limitations due to substrate availability and light affected the realised rate. All parameter choices were informed by field and laboratory studies and a detailed description is provided in the Supplementary Text S1.

New nitrogen is added to the ocean via biological nitrogen fixation, riverine fluxes, and atmospheric deposition. Nitrogen fixation and static riverine additions are equivalent to that presented in Aumont et al. (2015) and atmospheric deposition is maintained at preindustrial rates according to Hauglustaine et al. (2014) and applied as in Buchanan et al. (2021). Nitrogen is removed from the ocean via denitrification, anaerobic ammonium oxidation (anammox) and burial. The internal cycling of nitrogen involves assimilation by phytoplankton in particulate organic matter, grazing and excretion by zooplankton, solubilization of particulates to dissolved organics, ammonification of dissolved organic matter to  $\text{NH}_4^+$ , followed by nitrification of  $\text{NH}_4^+$  and  $\text{NO}_2^-$  via ammonia oxidation and nitrite oxidation (Supplementary Text S1)."

Lines 187 - 243: "2.2.2 Isolating the effect of competition for  $\text{NH}_4^+$

A unique aspect of the PISCESv2 biogeochemical model is that it weights uptake of  $\text{NH}_4^+$  over  $\text{NO}_3^-$  when both substrates are low, but as  $\text{NO}_3^-$  becomes abundant, the community switches towards using  $\text{NO}_3^-$  as a primary fuel (Fig. 2). This is achieved via

$$l_{\text{PFT}}^{\text{NH}_4^+} = \frac{[\text{NH}_4^+]}{[\text{NH}_4^+] + K_{\text{PFT}}^{\text{N}}} \quad (1)$$

$$l_{\text{PFT}}^{\text{NO}_x^-} = \frac{[\text{NO}_2^-] + [\text{NO}_3^-]}{[\text{NO}_2^-] + [\text{NO}_3^-] + K_{\text{PFT}}^{\text{N}}} \quad (2)$$

$$l_{\text{PFT}}^{\text{DIN}} = \frac{[\text{NH}_4^+] + [\text{NO}_2^-] + [\text{NO}_3^-]}{[\text{NH}_4^+] + [\text{NO}_2^-] + [\text{NO}_3^-] + K_{\text{PFT}}^{\text{N}}} \quad (3)$$

$$L_{\text{PFT}}^{\text{NH}_4^+} = \frac{5 \cdot l_{\text{PFT}}^{\text{DIN}} \cdot l_{\text{PFT}}^{\text{NH}_4^+}}{l_{\text{PFT}}^{\text{NO}_3^-} + 5 \cdot l_{\text{PFT}}^{\text{NH}_4^+}} \quad (4)$$

$$L_{\text{PFT}}^{\text{NO}_x^-} = \frac{l_{\text{PFT}}^{\text{DIN}} \cdot l_{\text{PFT}}^{\text{NO}_x^-}}{l_{\text{PFT}}^{\text{NO}_3^-} + 5 \cdot l_{\text{PFT}}^{\text{NH}_4^+}} \quad (5)$$

Where  $K_{\text{PFT}}^{\text{N}}$  is the prescribed half-saturation coefficient for uptake of inorganic nitrogen for a given phytoplankton functional type (PFT);  $[\text{NH}_4^+]$ ,  $[\text{NO}_2^-]$ , and  $[\text{NO}_3^-]$  are the molar concentrations of ammonium, nitrite and nitrate;  $l_{\text{PFT}}^{\text{NH}_4^+}$ ,  $l_{\text{PFT}}^{\text{NO}_x^-}$  and  $l_{\text{PFT}}^{\text{DIN}}$  are the michaelis-menten uptake terms for  $\text{NH}_4^+$ , inorganic oxidised nitrogen (the sum of  $\text{NO}_2^-$  and  $\text{NO}_3^-$ ), and

DIN; and  $L_{PFT}^{NH_4^+}$  and  $L_{PFT}^{NO_3^-}$  are the growth limitation factors on  $NH_4^+$  and inorganic oxidised nitrogen. In the above, the resulting  $L_{PFT}^{NH_4^+}$  and  $L_{PFT}^{NO_3^-}$  terms (Eqs. 4-5) are influenced by a factor 5 that is applied to  $L_{PFT}^{NH_4^+}$ . This assumes that  $NH_4^+$  uptake is weighted five times more than oxidised inorganic nitrogen, which represents the well-established preference for growth on  $NH_4^+$  (Dortch, 1990). However, as oxidised nitrogen (hereafter  $NO_3^-$ ) becomes more abundant than  $NH_4^+$  (specifically 5-times more abundant), the  $L_{PFT}^{NO_3^-}$  term exceeds  $L_{PFT}^{NH_4^+}$ , meaning that phytoplankton switch to new production over regenerated production (see cross over points between solid and dashed lines in Fig. 2).

These dynamics are common to both PFTs: nanophytoplankton and diatoms (Fig. 2). However, a key difference is that the  $K_{PFT}^N$  of diatoms is 3-fold greater than that of nanophytoplankton, reflecting their greater average size. As a result, diatoms are always less competitive than nanophytoplankton for  $NH_4^+$ , and are less competitive for  $NO_3^-$  when  $NO_3^-$  is scarce. However, a low  $L_{PFT}^{NH_4^+}$  for diatoms also results in a higher  $L_{PFT}^{NO_3^-}$  as  $NO_3^-$  concentrations rise. This is evident in Figure 2, where growth by diatoms on  $NO_3^-$  (black solid line) overtakes growth by nanophytoplankton on  $NO_3^-$  (green solid line) as  $NO_3^-$  becomes abundant. As a result, the model gives diatoms a competitive advantage over nanophytoplankton that accords with theorized growth advantages under high  $NO_3^-$  (Glibert et al., 2016a; Lomas and Glibert, 1999; Parker and Armbrust, 2005). Additionally, the switch from regenerated to new primary production occurs at much lower concentrations of  $NO_3^-$  for diatoms, aligning with field studies that identify diatoms as responsible for the majority of  $NO_3^-$  uptake in the nitracline (Fawcett et al., 2011).

We sought to isolate the impact of competition for  $NH_4^+$  and thus target the causative relationship between  $NH_4^+$ :DIN and variations in PFT relative abundance. To do so, we repeated the set of experiments described above (All, Phys, Warm and OA) but with an alternative parameterization where diatoms were made to have the same growth limitation on  $NH_4^+$  as other phytoplankton, so that there was zero competitive advantage or disadvantage for  $NH_4^+$  between these groups. This simulation was called “model<sub>compete</sub>” and was equivalent to making the dashed black and green lines in Figure 2 the same under all conditions (see upward arrow in Fig. 2). All other traits remained unchanged. Importantly, this included the competitive advantage of diatoms at high  $NO_3^-$  but also their competitive disadvantage at low  $NO_3^-$ . In other words, when DIN was low, diatoms were equally competitive for  $NH_4^+$ , but still suffered their unique limitations associated with  $NO_3^-$ , light, silicate, phosphate, and iron availability, as well as grazing pressure. Meanwhile, “model<sub>control</sub>” used the default parameterization above.

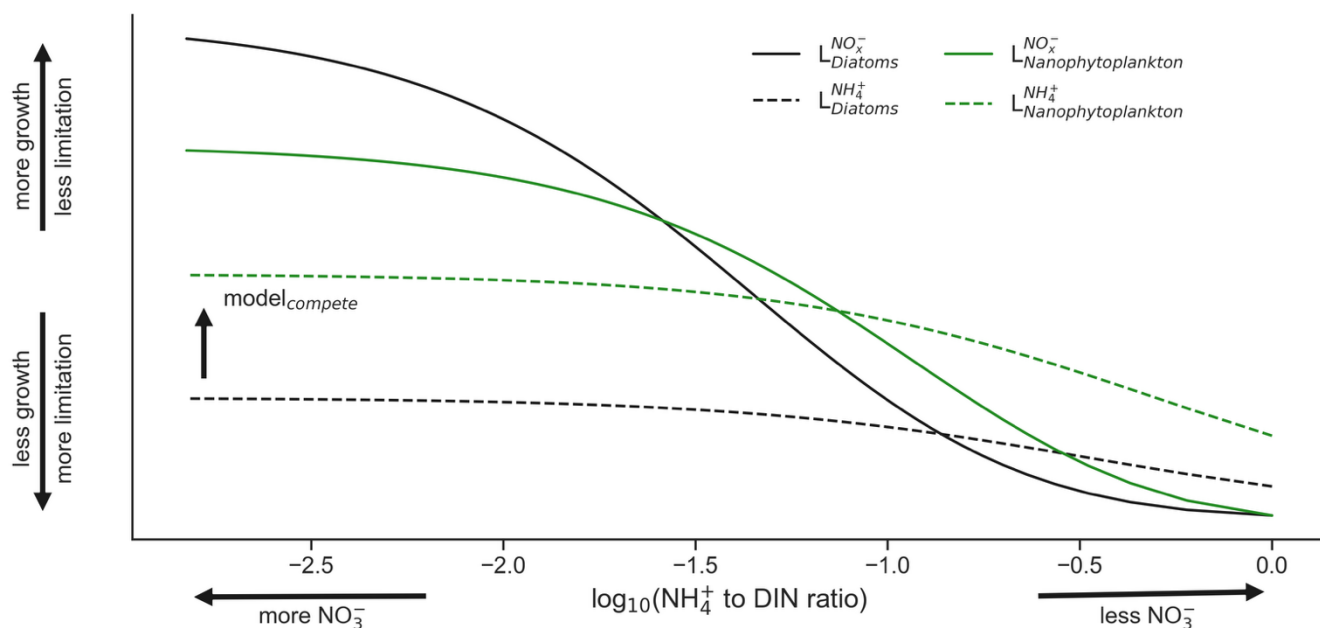


Figure 2. Limitation of the diatom (black) and nanophytoplankton (green) phytoplankton functional types (PFT) in the ocean-biogeochemical model by  $\text{NO}_3^-$  (solid lines) and  $\text{NH}_4^+$  (dashed lines) as a function of the  $\text{NH}_4^+:\text{DIN}$  ratio on a  $\log_{10}$  scale. Note that the nanophytoplankton PFT is always more competitive for  $\text{NH}_4^+$  and is more competitive for  $\text{NO}_3^-$  when  $\text{NO}_3^-$  is low, while diatoms become more competitive for  $\text{NO}_3^-$  when  $\text{NO}_3^-$  is high.”

### Lines 343-371: “3.1 Assessment of modelled $\text{NH}_4^+$ and $\text{NH}_4^+:\text{DIN}$

Concentrations of  $0.1 \mu\text{M}$   $\text{NH}_4^+$  or greater exist over continental shelves and in regions of strong mixing with high rates of primary production and subsequent heterotrophy. This accumulation of  $\text{NH}_4^+$  in productive regions is reproduced by our model (Fig. 3a). In these eutrophic systems, high  $\text{NH}_4^+$  co-occurs with high  $\text{NO}_3^-$  concentrations, so  $\text{NH}_4^+$  makes a small contribution to total DIN (Fig. 3b). These regions include the eastern tropical Pacific, eastern boundary upwelling systems, the northwest Indian Ocean, the subpolar gyres and the Southern Ocean (although we note that the model underestimates  $\text{NH}_4^+$  concentrations in the Southern Ocean). In contrast, low  $\text{NH}_4^+$  concentrations of less than  $0.05 \mu\text{M}$  pervade the oligotrophic gyres of the lower latitudes. As these regions also display very low  $\text{NO}_3^-$  concentrations,  $\text{NH}_4^+$  makes up a much higher fraction of total DIN in both the observations and our model, with the  $\text{NH}_4^+$  peak occurring deeper in the water column (Fig. S1).

Eutrophic upwelling systems and oligotrophic waters differed in the major sinks of  $\text{NH}_4^+$  (Fig. 3c), consistent with available observations and constraints from theory. In eutrophic waters (here defined by surface nitrate  $> 1 \mu\text{M}$ ), ammonia oxidation represented  $49 \pm 29 \%$  (mean  $\pm$  standard deviation) of  $\text{NH}_4^+$  sinks, but this dropped to  $32 \pm 9 \%$  in oligotrophic systems. Measured rates of ammonia oxidation showed a positive relationship with surface  $\text{NO}_3^-$  concentrations and this was reproduced by the model (Fig. S2), indicating that ammonia oxidation was indeed a greater proportion of the overall  $\text{NH}_4^+$  budget in eutrophic regions. In agreement, isotopic methods have shown that the bulk of nitrogen assimilated by phytoplankton in oligotrophic waters is recycled (Eppley and Peterson, 1979; Fawcett et al., 2011; Klawonn et al., 2019; Van Oostende et al., 2017; Wan et al., 2021), implying that most nitrogen cycling occurs without ammonia oxidation. Our model reproduces this feature of



oligotrophic systems (Fig. 3c). Overall, the model shows good fidelity to the available observations of  $\text{NH}_4^+$  concentrations,  $\text{NH}_4^+:\text{DIN}$  ratios, and rates of  $\text{NH}_4^+$  cycling that we compiled for this study (Fig. 3; Fig. S2-S3).

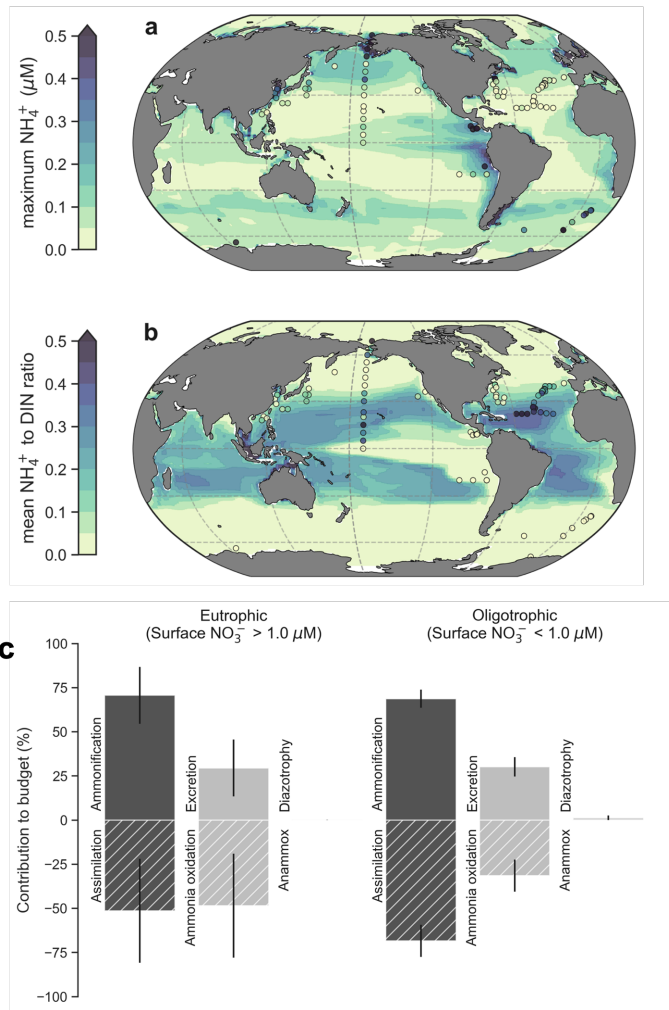


**Figure 3.** Global patterns of  $\text{NH}_4^+$  concentrations, its contribution to DIN in the euphotic zone, and  $\text{NH}_4^+$  budgets. (a) The simulated maximum  $\text{NH}_4^+$  concentration within the euphotic zone. The maximum was chosen to emphasise basin-scale variations. (b) Average values of the  $\text{NH}_4^+:\text{DIN}$  ratio. Modelled values are annual averages of the preindustrial control simulation between years 2081-2100. Observed values following linear interpolation between the surface and 200 metres depth are overlaid as coloured markers. Only those profiles with at least 3 data points within the upper 200 metres are shown. (c) Global mean  $\pm$  standard deviations of  $\text{NH}_4^+$  fluxes separated into eutrophic and oligotrophic regions. Sources of  $\text{NH}_4^+$  are represented by positive values and sinks by negative values.”

Fig. 3 shows a 70% difference in the decline of delta % diatoms between the Model<sub>control</sub> and Model<sub>compete</sub>. However, their delta  $\mu\text{M C}$  diatoms are very similar (Fig. S9). Could the changes in delta % diatoms during the transient simulation mainly result from differences in the initial conditions rather than the  $\text{NH}_4\text{:DIN}$  ratio? If so, the decline in delta % diatoms might be primarily driven by a decrease in the overall nutrient pool rather than by competition with nanophytoplankton.

We appreciate the reviewer's question about this detail and we have improved our clarity in the methods. Our methods fully isolate the effect of competition for  $\text{NH}_4^+$  on diatom relative abundance.

Lines 151 - 237:

#### *“2.2.1 Identifying anthropogenic drivers*

*To quantify the impact of anthropogenic activities on  $\text{NH}_4^+\text{:DIN}$  ratios, we performed transient simulations by forcing the biogeochemical model with monthly physical outputs (temperature, salinity, ocean transports, short wave radiation and wind speeds) produced by the Institut Pierre-Simon Laplace Climate Model 5A (Dufresne et al., 2013). Simulations included a preindustrial control (years 1850 to 2100) where land-use, greenhouse gases and ozone remained at preindustrial conditions, and a climate change run (years 1850 to 2100) where these factors changed according to historical observations from 1850 to 2005 and according to the high emissions Representative Concentration Pathway 8.5 from 2006 to 2100 (RCP8.5) (Riahi et al., 2011). We chose a high emissions scenario to emphasize the clearest degree of anthropogenic changes and thus maximize anthropogenic effects. However, we acknowledge that the RCP8.5 is considered an extreme scenario under present development pathways (Riahi et al., 2017).*

*In addition, we performed parallel experiments (years 1850 to 2100) that isolated the individual effects of our three anthropogenic stressors: a changing circulation (“Phys”), warming on biological metabolism (“Warm”), and acidification effects on ammonia oxidation (“OA”). The experiment with all anthropogenic effects was termed “All”. These experiments involved altering the factor of interest in line with the historical and RCP8.5 scenario while holding the other factors at their preindustrial state. Experiment “Phys”, for example, involved changing the ocean’s circulation, temperature and salinity, and the resulting effects to light associated with sea-ice extent changes, but the ecosystem component of the model experienced only the preindustrial temperature, and atmospheric  $\text{CO}_2$  was held at a preindustrial concentration of 284 ppm. In contrast, experiment “Warm” maintained the preindustrial climatological ocean state and atmospheric  $\text{CO}_2$  at 284 ppm, but ensured that the ecosystem component saw increasing temperatures ( $T$  in  $^\circ\text{C}$ ) according to the RCP8.5 scenario, which scaled growth of phytoplankton types according to  $1.066^T$  and heterotrophic activity (grazing and remineralisation) according to  $1.079^T$  (Aumont et al., 2015). Experiment “OA” held the circulation and temperature effects on metabolism constant but involved the historical and future projected increase in atmospheric  $\text{CO}_2$ . This decreased pH and negatively affected rates of ammonia oxidation at a rate consistent with field measurements (Beman et al., 2011; Huesemann et al., 2002; Kitidis et al., 2011), specifically a loss of  $\sim 20\%$  per 0.1 unit decrease in pH below 8.0 (Fig. S1).*

*The effect of climate change at the end of the 21<sup>st</sup> century (mean conditions 2081-2100) was quantified by comparing with the preindustrial control simulation (also mean conditions*

2081-2100). This preindustrial control simulation was run parallel to the climate change simulations (i.e., 1850-2100), but without anthropogenic forcings. This allowed a direct comparison to be made between experiments at the end of the 21<sup>st</sup> century and eliminated the effect of model drift. We calculated changes at each grid cell by averaging over the upper ocean where primary production was active, which was defined as those depths where total phytoplankton biomass was greater than 0.1 mmol C m<sup>-3</sup>. In addition, we compared the preindustrial simulation with observations to explore broad patterns in NH<sub>4</sub><sup>+</sup> and NH<sub>4</sub><sup>+</sup>:DIN ratios.

### 2.2.2 Isolating the effect of competition for NH<sub>4</sub><sup>+</sup>

A unique aspect of the PISCESv2 biogeochemical model is that it weights uptake of NH<sub>4</sub><sup>+</sup> over NO<sub>3</sub><sup>-</sup> when both substrates are low, but as NO<sub>3</sub><sup>-</sup> becomes abundant, the community switches towards using NO<sub>3</sub><sup>-</sup> as a primary fuel (Fig. 2). This is achieved via

$$l_{PFT}^{NH_4^+} = \frac{[NH_4^+]}{[NH_4^+] + K_{PFT}^N} \quad (1)$$

$$l_{PFT}^{NO_x^-} = \frac{[NO_2^-] + [NO_3^-]}{[NO_2^-] + [NO_3^-] + K_{PFT}^N} \quad (2)$$

$$l_{PFT}^{DIN} = \frac{[NH_4^+] + [NO_2^-] + [NO_3^-]}{[NH_4^+] + [NO_2^-] + [NO_3^-] + K_{PFT}^N} \quad (3)$$

$$L_{PFT}^{NH_4^+} = \frac{5 \cdot l_{PFT}^{DIN} \cdot l_{PFT}^{NH_4^+}}{l_{PFT}^{NO_3^-} + 5 \cdot l_{PFT}^{NH_4^+}} \quad (4)$$

$$L_{PFT}^{NO_x^-} = \frac{l_{PFT}^{DIN} \cdot l_{PFT}^{NO_x^-}}{l_{PFT}^{NO_3^-} + 5 \cdot l_{PFT}^{NH_4^+}} \quad (5)$$

Where  $K_{PFT}^N$  is the prescribed half-saturation coefficient for uptake of inorganic nitrogen for a given phytoplankton functional type (PFT);  $[NH_4^+]$ ,  $[NO_2^-]$ , and  $[NO_3^-]$  are the molar concentrations of ammonium, nitrite and nitrate;  $l_{PFT}^{NH_4^+}$ ,  $l_{PFT}^{NO_x^-}$  and  $l_{PFT}^{DIN}$  are the michaelis-menten uptake terms for NH<sub>4</sub><sup>+</sup>, inorganic oxidised nitrogen (the sum of NO<sub>2</sub><sup>-</sup> and NO<sub>3</sub><sup>-</sup>), and DIN; and  $L_{PFT}^{NH_4^+}$  and  $L_{PFT}^{NO_x^-}$  are the growth limitation factors on NH<sub>4</sub><sup>+</sup> and inorganic oxidised nitrogen. In the above, the resulting  $L_{PFT}^{NH_4^+}$  and  $L_{PFT}^{NO_x^-}$  terms (Eqs. 4-5) are influenced by a factor 5 that is applied to  $l_{PFT}^{NH_4^+}$ . This assumes that NH<sub>4</sub><sup>+</sup> uptake is weighted five times more than oxidised inorganic nitrogen, which represents the well-established preference for growth on NH<sub>4</sub><sup>+</sup> (Dortch, 1990). However, as oxidised nitrogen (hereafter NO<sub>3</sub><sup>-</sup>) becomes more abundant than NH<sub>4</sub><sup>+</sup>, the  $L_{PFT}^{NO_x^-}$  term exceeds  $L_{PFT}^{NH_4^+}$ , meaning that phytoplankton switch to new production over regenerated production (see cross over points between solid and dashed lines in Fig. 2).

These dynamics are common to both PFTs: nanophytoplankton and diatoms (Fig. 2). However, a key difference is that the  $K_{PFT}^N$  of diatoms is prescribed as 3-fold greater than that of nanophytoplankton, reflecting their greater average size. As a result, diatoms are always less competitive than nanophytoplankton for NH<sub>4</sub><sup>+</sup> and are less competitive for NO<sub>3</sub><sup>-</sup> when NO<sub>3</sub><sup>-</sup> is scarce. However, a low  $l_{PFT}^{NH_4^+}$  for diatoms also results in a higher  $L_{PFT}^{NO_x^-}$  as NO<sub>3</sub><sup>-</sup> concentrations rise. This is evident in Figure 2, where growth by diatoms on NO<sub>3</sub><sup>-</sup> (black



solid line) overtakes growth by nanophytoplankton on  $\text{NO}_3^-$  (green solid line) as  $\text{NO}_3^-$  becomes abundant. As a result, the model gives diatoms a competitive advantage over nanophytoplankton that accords with theorized growth advantages under high  $\text{NO}_3^-$  (Glibert et al., 2016a; Lomas and Glibert, 1999; Parker and Armbrust, 2005). Additionally, the switch from regenerated to new primary production occurs at much lower concentrations of  $\text{NO}_3^-$  for diatoms, aligning with fields studies that identify diatoms as responsible for the majority of  $\text{NO}_3^-$  uptake in the nitracline (Fawcett et al., 2011).

We sought to isolate the impact of competition for  $\text{NH}_4^+$  and thus target the causative relationship between  $\text{NH}_4^+:\text{DIN}$  and variations in PFT relative abundance. To do so, we repeated the set of experiments described above (All, Phys, Warm, OA and the preindustrial control) from years 1850 to 2100 but with an alternative parameterization where diatoms were made to have the same growth limitation on  $\text{NH}_4^+$  as other phytoplankton, so that there was zero competitive advantage or disadvantage for  $\text{NH}_4^+$  between these groups (i.e., making the dashed black and green lines in Figure 2 the same under all conditions). These simulations were completed with “model<sub>compete</sub>” and were initialised from the same conditions as those done with the default parameterisation, which we call “model<sub>control</sub>”. All other traits remained unchanged. Importantly, this included the competitive advantage of diatoms at high  $\text{NO}_3^-$  but also their competitive disadvantage at low  $\text{NO}_3^-$  (Fig. 2). In other words, when DIN was low, diatoms were equally competitive for  $\text{NH}_4^+$ , but still suffered their unique limitations associated with  $\text{NO}_3^-$ , light, silicate, phosphate, and iron availability, as well as grazing pressure, and this isolated the direct effect of competition for  $\text{NH}_4^+$ .

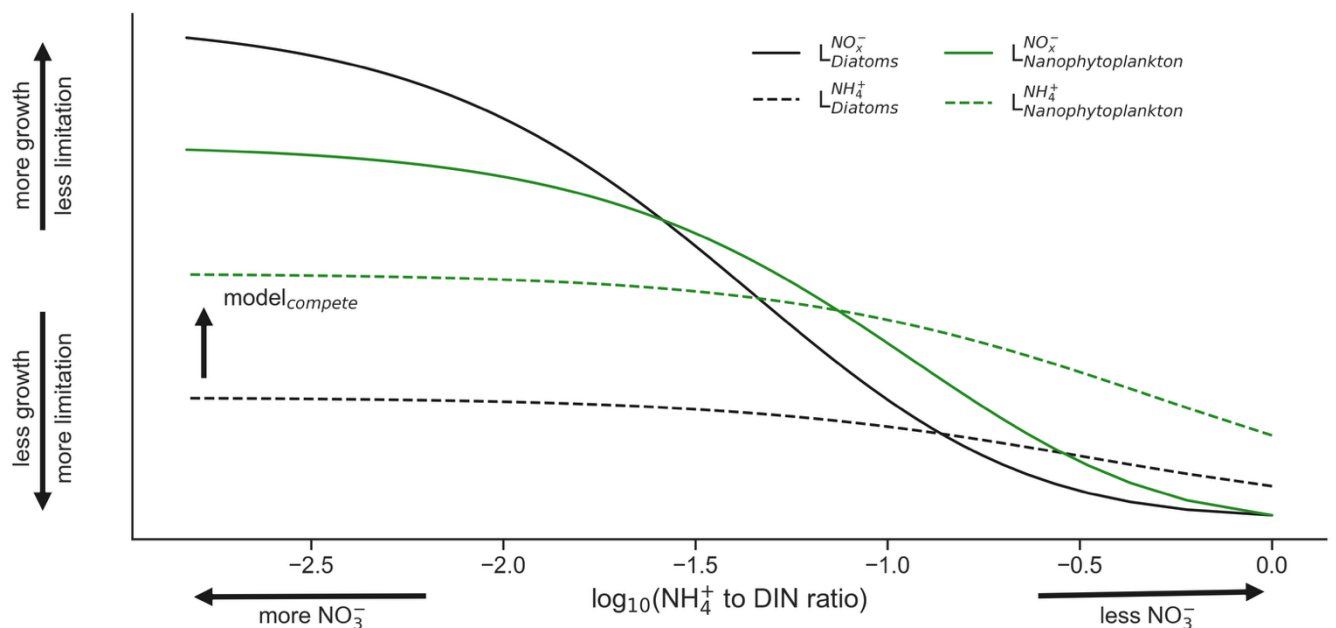


**Figure 2.** Limitation of the diatom (black) and nanophytoplankton (green) phytoplankton functional types (PFT) in the ocean-biogeochemical model by  $\text{NO}_3^-$  (solid lines) and  $\text{NH}_4^+$  (dashed lines) as a function of the  $\text{NH}_4^+:\text{DIN}$  ratio on a  $\log_{10}$  scale. Note that the nanophytoplankton PFT is always more competitive for  $\text{NH}_4^+$  and is more competitive for  $\text{NO}_3^-$  when  $\text{NO}_3^-$  is low, while diatoms become more competitive for  $\text{NO}_3^-$  when  $\text{NO}_3^-$  is high.”

This brings another question to me. The manuscript does not discuss nanophytoplankton abundance during the transient simulations. Is the decline in their abundance really smaller than that of diatoms by the end of this century?

Yes this is correct. And that is why diatom relative abundance declines.

From Fig. S8a, the “delta other phytoplankton” are negative in most of the low latitude regions, where the NH<sub>4</sub>:DIN increases mostly. Since the title highlights impacts on phytoplankton community composition, I believe this is an important point. More discussion is needed on how both phytoplankton groups respond to the NH<sub>4</sub>:DIN shift.

We agree with the reviewer that this is an important point. As such, we discuss openly in the paper that the biomass and productivity of phytoplankton declines in general outside of the polar environments:

Lines 483 - 485:

*“We indeed appreciate that the reduction of diatoms from phytoplankton communities as simulated by models is due to nutrient losses, in particular declines in NO<sub>3</sub><sup>-</sup> (Kwiatkowski et al., 2020), and our simulations here, at least indirectly, are no different, since both nanophytoplankton and diatom biomass declined.”*

Lines 560 - 563:

*“Losses in NO<sub>3</sub><sup>-</sup> still occurred in these experiments, and these losses in NO<sub>3</sub><sup>-</sup> caused declines in phytoplankton productivity and biomass, including both nanophytoplankton and diatoms everywhere outside of the polar regions (Fig. S7-S8). In the default model (model<sub>control</sub>) diatoms experienced greater declines than nanophytoplankton, causing losses in relative abundance.”*

Specific comments

Title: The majority of changes in diatom abundance due to changes in the NH<sub>4</sub>:NO<sub>3</sub> ratio occur in trophic and subtropic regions (Fig. 3a and d), where NH<sub>4</sub> concentration actually decreases (Fig. S6). Therefore, I suggest revising the phrase “enrichment of ammonium” in the title, as it may not accurately reflect the spatial trends shown in the results.

We have changed the title to avoid confusion from:

“Oceanic enrichment of ammonium and its impacts on phytoplankton community composition under a high-emissions scenario”,

to:

“Relative enrichment of ammonium and its impacts on open-ocean phytoplankton community composition under a high-emissions scenario”,

Line 27: an -> a

Corrected.

Line 30: remove the extra “in”

Corrected.

Fig. 1: Suggest adding labels to indicate which conditions are subject to anthropogenic pressure.

All processes are subject to anthropogenic climate change and resulting property changes. To make this more explicit, we have added a note to the figure legend: *“All processes are affected by changes to seawater properties driven by large-scale climate change.”*

Line 101: Are riverine inputs and nitrogen deposition influenced by anthropogenic forcing in the model?

Good question! No they are not and we have made this explicit in the methods:

Lines 124 – 126:

*“New nitrogen is added to the ocean via biological nitrogen fixation, riverine fluxes, and atmospheric deposition. Nitrogen fixation and static riverine additions are equivalent to that presented in Aumont et al. (2015) and atmospheric deposition is maintained at preindustrial rates according to Hauglustaine et al. (2014) and applied as in Buchanan et al. (2021).”*

Line 104-108: As mentioned in the major comments, please include some evaluations here, particularly for the nitrogen fixation since it's also affected by the forcings. Additionally, I couldn't find the information regarding the form of N introduced to the system through nitrogen fixation.

We have expanded our description of the nitrogen cycle within this version of PISCESv2 to address the reviewers request. This expansion reads as:

Lines 104 – 130:

*“The biogeochemical model is the Pelagic Interactions Scheme for Carbon and Ecosystem Studies version 2 (PISCES-v2), which is detailed and assessed in Aumont et al. (2015). This model is embedded within version 4.0 of the Nucleus for European Modelling of the Ocean (NEMO-v4.0). We chose a 2° nominal horizontal resolution with 31 vertical levels with thicknesses ranging from 10 meters in the upper 100 meters to 500 meters below 2000 meters. Due to the curvilinear grid, horizontal resolution increases to 0.5° at the equator and to near 1° poleward of 50°N and 50°S.*

*We updated the standard PISCES-v2 (Aumont et al., 2015) for the purposes of this study, specifically by adding  $\text{NO}_2^-$  as a new tracer. The PISCESv2 biogeochemical model already resolved the pools of  $\text{NH}_4^+$ ,  $\text{NO}_3^-$ , dissolved oxygen, the carbon system, dissolved iron, phosphate, two kinds of phytoplankton biomass (nanophytoplankton and diatoms), two kinds of zooplankton biomass (micro- and meso-zooplankton), small and large pools of particulate organic matter, and dissolved organic matter (Aumont et al., 2015). The addition of  $\text{NO}_2^-$  necessitated breaking full nitrification ( $\text{NH}_4^+ \rightarrow \text{NO}_3^-$ ) into its two steps of ammonia ( $\text{NH}_4^+ \rightarrow \text{NO}_2^-$ ) and nitrite oxidation ( $\text{NO}_2^- \rightarrow \text{NO}_3^-$ ). Both steps were simulated implicitly by multiplying a maximum growth rate by the concentration of substrate and limitation terms representing the effect of environmental conditions to return the realized rate. For ammonia oxidation, limitations due to substrate availability, light and pH determined the realised rate. For nitrite oxidation, limitations due to substrate availability and light affected the realised rate. All parameter choices were informed by field and laboratory studies and a detailed description is provided in the Supplementary Text S1.*

*New nitrogen is added to the ocean via biological nitrogen fixation, riverine fluxes, and atmospheric deposition. Nitrogen fixation and static riverine additions are equivalent to that presented in Aumont et al. (2015) and atmospheric deposition is maintained at preindustrial rates according to Hauglustaine et al. (2014) and applied as in Buchanan et al. (2021). Nitrogen is removed from the ocean via denitrification, anaerobic ammonium oxidation (anammox) and burial. The internal cycling of nitrogen involves assimilation by phytoplankton in particulate organic matter, grazing and excretion by zooplankton, solubilization of particulates to dissolved organics, ammonification of dissolved organic matter to  $\text{NH}_4^+$ , followed by nitrification of  $\text{NH}_4^+$  and  $\text{NO}_2^-$  via ammonia oxidation and nitrite oxidation (Supplementary Text S1). “*

With regard to the effect of nitrogen fixation, its contribution to nitrogen cycling is now showcased in what is now Figure 3c.

Line 121: Please provide a clearer description of the “changing circulation (‘Phys’)” configuration. For example, does it include stronger stratification? It is not clear which specific factors are incorporated under this forcing. Later in the text (Line 211), changes in sea-ice loss are also mentioned as part of this forcing, so clarification is needed regarding which processes are included.

To address the reviewers concern, we have expanded on this paragraph to explain more fully what the sensitivity experiments were composed of:

Lines 166 – 175:

*“Experiment ‘Phys’, for example, involved changing the ocean’s circulation, temperature and salinity, and the resulting effects to light associated with sea-ice extent changes, but the ecosystem component of the model experienced only the preindustrial temperature, and atmospheric  $\text{CO}_2$  was held at a preindustrial concentration of 284 ppm. In contrast, experiment ‘Warm’ maintained the preindustrial climatological ocean state and atmospheric  $\text{CO}_2$  at 284 ppm, but ensured that the ecosystem component saw increasing temperatures ( $T$  in  $^\circ\text{C}$ ) according to the RCP8.5 scenario, which scaled growth of phytoplankton types according to  $1.066^T$  and heterotrophic activity (grazing and remineralisation) according to  $1.079^T$  (Aumont et al., 2015). Experiment ‘OA’ held the circulation and temperature effects on metabolism constant but involved the historical and future projected increase in atmospheric  $\text{CO}_2$ . This decreased pH and negatively affected rates of ammonia oxidation at a rate consistent with field measurements (Beman et al., 2011; Huesemann et al., 2002; Kitidis et al., 2011), specifically a loss of ~20% per 0.1 unit decrease in pH below 8.0 (Fig. S1).”*

Line 129: Please provide a reference or justification for this criterion ( $0.1 \text{ mmol C m}^{-3}$ ).

We have removed the reference to the “euphotic zone” here to avoid confusion. The sentence now reads:

Lines 181 – 185:

*“We calculated changes at each grid cell by averaging over the upper ocean where primary production was active, which was defined as those depths where total phytoplankton biomass was greater than  $0.1 \text{ mmol C m}^{-3}$ .”*

Line 160-163: Why the rate saturates when  $\text{pH} > 8$ ? Base on the equation in Fig. S5 the rate is supposed to keep increase.

We chose a pH value where pH is no longer limiting to the maximum possible rate of ammonia oxidation, but beneath which ammonia oxidation becomes limited by pH declines as more  $\text{NH}_3$  is converted to  $\text{NH}_4^+$ . Figure S5 (now Fig. S1) clearly shows this cut off, but we acknowledge that this was not clear in the equation within Figure S5 (now Fig. S1). We have rectified this inconsistency by including a new equation to the figure. We also updated the equations in Fig. S6.

Equation (1): at least one item is missing before  $+s_1(x_1)$ .

Corrected.

Line 183: the intercept  $\alpha$  is missing in the equation.

Corrected.

Line 183: “thin-plate spline” is not a trivial term, it would be helpful if the author could provide a brief explanation or background information in the text.

We agree that this necessitates a bit more explanation:

Lines 295 – 299:

*“Where  $Y$  is the predicted response,  $\alpha$  is the intercept,  $s_n(x_n)$  represents a smooth function (specifically the  $n^{\text{th}}$  thin-plate spline) fitted to the  $n^{\text{th}}$  predictor variable  $x_n$ , and  $\varepsilon$  is the model error. Thin-plate splines are flexible and widely used as a smoothing method within GAMs that allow for non-linear relationships between predictors and response variables and do not require specificity around a functional form. They are well suited to handling ecological data where relationships are often non-linear and non-parametric.”*

Line 184: independent variable. -> independent variable  $x$ .

Corrected.

Line 193-194: Please provide a bit more information regarding the VIFs and the criterion.

Addressed.

*“All covariate VIFs were  $< 3$ , which indicates minimal multicollinearity.”*

Line 210-211: The full name was mentioned in the Methods and it is sufficient using only RCP8.5 here.

This has been removed.

Line 211: “sea-ice loss” should be mentioned already in the methods instead of here.

This has been mentioned now on line 167. We thank the reviewer for catching this.

Line 217: What does the  $\pm 6$  stands for?

standard deviation. Clarified in the text.



Line 219: Please give specific locations for examples for the “oceanographic fronts”.  
replaced on line 371 by *“as at the boundary between eutrophic and oligotrophic regimes”*

Line 225-242: When comparing Fig. 3b and 3e, the major contribution to the changes in diatom abundance appears to come from the "phys", which aligns with its 55% contribution to the  $\text{NH}_4\text{:NO}_3$  ratio. However, although the contribution from OA (25%) is about double that of Warming (13%), OA appears to have almost no effect on the changes in diatom between Fig. 3b and 3e. This discrepancy should be addressed and further explained in the manuscript.

We completely agree with the reviewer and we have allocated an explanatory sentence to this result:

Lines 472 – 476:

*“At a global scale, the loss of diatom representation within marine communities in our model was driven by a combination of stimulated microbial metabolism (60% of full response in experiment “All”) and physical changes (40% of full response in experiment “All”), while ocean acidification had negligible effects (Figure 5c; Fig. S7). Ocean acidification had negligible effects because it largely raised  $\text{NH}_4^+:\text{DIN}$  ratios in oligotrophic subtropical gyres where diatoms were already of low proportion (Fig. 4c; Fig. S5).”*

Fig. 3 and Fig. S9: The delta  $\mu\text{M C}$  diatoms of “All” are comparable between  $\text{Model}_{\text{control}}$  and  $\text{Model}_{\text{compete}}$  in Fig. S9, yet the delta % diatoms in Fig. 3 show much larger difference. Does this imply that the total diatom biomass is substantially higher in  $\text{Model}_{\text{compete}}$ ? Additionally, in  $\text{Model}_{\text{control}}$ , the delta  $\mu\text{M C}$  diatoms decline under “Warm” is about 2.5 times greater than Phys (Fig. S9c), but their delta % diatoms declines are similar. Does this indicate that the diatom biomass is much higher in “Phys”? These discrepancies should be clarified in the text, as they are important for interpreting the results.

The reviewer brings attention to an important nuance of the results: that both diatom and nanophytoplankton biomass decrease in the “All” experiment in both  $\text{model}_{\text{control}}$  and  $\text{model}_{\text{compete}}$  experiments, but that the diatom relative abundance decreased much less in  $\text{model}_{\text{compete}}$ . This means that diatoms still decrease in  $\text{model}_{\text{compete}}$  and their losses were greater than nanophytoplankton losses, but to a much lesser extent than in  $\text{model}_{\text{control}}$ .

We have clarified this nuance in the text:

Lines 558 – 571:

*“Removing diatoms competitive disadvantage for  $\text{NH}_4^+$  (i.e., equally competitive for  $\text{NH}_4^+$ ) in our experiments with “ $\text{model}_{\text{compete}}$ ” (see section 2.2.2 in the methods) mitigated the losses of diatom representation within future phytoplankton communities by 70% compared to the full response in the “All” experiment with  $\text{model}_{\text{control}}$  (Fig. 5d-f). Losses in  $\text{NO}_3^-$  still occurred in these experiments, and these losses in  $\text{NO}_3^-$  caused declines in phytoplankton productivity and biomass, including both nanophytoplankton and diatoms everywhere outside of the polar regions (Fig. S7-S8). In the default model ( $\text{model}_{\text{control}}$ ) diatoms experienced greater declines than nanophytoplankton, causing declines in their relative abundance. Importantly though, the global mean decline in diatom relative abundance in  $\text{model}_{\text{compete}}$  was only 0.9% by 2081-2100 compared to 3% in  $\text{model}_{\text{control}}$  (Fig. 5c,f). Physical changes, while important regionally,*

*no longer exerted a global negative effect on their total nor relative abundance (blue line in Fig. 5f), while the negative effect of elevated microbial metabolism on relative abundance was ameliorated by 25% (Fig. 5f; Fig. S7-S8). In some areas diatoms even showed increased total and/or relative abundance where previously there were losses, including the Arctic, the tropical Pacific, the Arabian Sea, the North Atlantic, and the southern subtropics (Fig. 5d,e; Fig. S8). Outside of the Southern Ocean and the eastern boundary upwelling systems, physical changes that tended to reduce DIN concentrations now favoured diatoms, while elevated metabolism now had positive, rather than negative, effects in the tropical Pacific.”*

In relation to this comment by the reviewer: “Additionally, in Model<sub>control</sub>, the delta  $\mu\text{M C}$  diatoms decline under “Warm” is about 2.5 times greater than Phys (Fig. S9c), but their delta % diatoms declines are similar. Does this indicate that the diatom biomass is much higher in “Phys”?” we stress that the changes in diatom relative abundance are not dependent on the changes in absolute PFT biomass, as it depends entirely on how much nanophytoplankton change in relation to diatoms. So in experiment “Warm”, the declines in diatom and nanophytoplankton biomass are indeed stronger than in “Phys”, but because in both cases the relative declines are similar, both “Phys” and “warm” have similar effects on the relative abundance of diatoms.

We feel that the revised text in the methods has clarified these points and resolved any prior ambiguities.

Line 289: thid -> the or this?

Corrected.

Line 296-304: move to method. Also, was the model<sub>compete</sub> simulation spun up before the transient simulation? Such information is missing in the text.

We agree! We have created a new methods section that is focussed on these experiments and also explains the nitrogen limitation function in PISCESv2. This reads as follows:

Lines 184 – 237:

*“2.2.2 Isolating the effect of competition for  $\text{NH}_4^+$*

*A unique aspect of the PISCESv2 biogeochemical model is that it weights uptake of  $\text{NH}_4^+$  over  $\text{NO}_3^-$  when both substrates are low, but as  $\text{NO}_3^-$  becomes abundant, the community switches towards using  $\text{NO}_3^-$  as a primary fuel (Fig. 2). This is achieved via*

$$l_{PFT}^{\text{NH}_4^+} = \frac{[\text{NH}_4^+]}{[\text{NH}_4^+] + K_{PFT}^N} \quad (1)$$

$$l_{PFT}^{\text{NO}_3^-} = \frac{[\text{NO}_2^-] + [\text{NO}_3^-]}{[\text{NO}_2^-] + [\text{NO}_3^-] + K_{PFT}^N} \quad (2)$$

$$l_{PFT}^{\text{DIN}} = \frac{[\text{NH}_4^+] + [\text{NO}_2^-] + [\text{NO}_3^-]}{[\text{NH}_4^+] + [\text{NO}_2^-] + [\text{NO}_3^-] + K_{PFT}^N} \quad (3)$$

$$L_{PFT}^{NH_4^+} = \frac{5 \cdot l_{PFT}^{DIN} \cdot l_{PFT}^{NH_4^+}}{l_{PFT}^{NO_3^-} + 5 \cdot l_{PFT}^{NH_4^+}} \quad (4)$$

$$L_{PFT}^{NO_x^-} = \frac{l_{PFT}^{DIN} \cdot l_{PFT}^{NO_x^-}}{l_{PFT}^{NO_3^-} + 5 \cdot l_{PFT}^{NH_4^+}} \quad (5)$$

Where  $K_{PFT}^N$  is the prescribed half-saturation coefficient for uptake of inorganic nitrogen for a given phytoplankton functional type (PFT);  $[NH_4^+]$ ,  $[NO_2^-]$ , and  $[NO_3^-]$  are the molar concentrations of ammonium, nitrite and nitrate;  $l_{PFT}^{NH_4^+}$ ,  $l_{PFT}^{NO_x^-}$  and  $l_{PFT}^{DIN}$  are the michaelis-menten uptake terms for  $NH_4^+$ , inorganic oxidised nitrogen (the sum of  $NO_2^-$  and  $NO_3^-$ ), and DIN; and  $L_{PFT}^{NH_4^+}$  and  $L_{PFT}^{NO_x^-}$  are the growth limitation factors on  $NH_4^+$  and inorganic oxidised nitrogen. In the above, the resulting  $L_{PFT}^{NH_4^+}$  and  $L_{PFT}^{NO_x^-}$  terms (Eqs. 4-5) are influenced by a factor 5 that is applied to  $l_{PFT}^{NH_4^+}$ . This assumes that  $NH_4^+$  uptake is weighted five times more than oxidised inorganic nitrogen, which represents the well-established preference for growth on  $NH_4^+$  (Dortch, 1990). However, as oxidised nitrogen (hereafter  $NO_3^-$ ) becomes more abundant than  $NH_4^+$  (specifically 5-times more abundant), the  $L_{PFT}^{NO_x^-}$  term exceeds  $L_{PFT}^{NH_4^+}$ , meaning that phytoplankton switch to new production over regenerated production (see cross over points between solid and dashed lines in Fig. 2).

These dynamics are common to both PFTs: nanophytoplankton and diatoms (Fig. 2). However, a key difference is that the  $K_{PFT}^N$  of diatoms is 3-fold greater than that of nanophytoplankton, reflecting their greater average size. As a result, diatoms are always less competitive than nanophytoplankton for  $NH_4^+$ , and are less competitive for  $NO_3^-$  when  $NO_3^-$  is scarce. However, a low  $l_{PFT}^{NH_4^+}$  for diatoms also results in a higher  $L_{PFT}^{NO_x^-}$  as  $NO_3^-$  concentrations rise. This is evident in Figure 2, where growth by diatoms on  $NO_3^-$  (black solid line) overtakes growth by nanophytoplankton on  $NO_3^-$  (green solid line) as  $NO_3^-$  becomes abundant. As a result, the model gives diatoms a competitive advantage over nanophytoplankton that accords with theorized growth advantages under high  $NO_3^-$  (Glibert et al., 2016a; Lomas and Glibert, 1999; Parker and Armbrust, 2005). Additionally, the switch from regenerated to new primary production occurs at much lower concentrations of  $NO_3^-$  for diatoms, aligning with field studies that identify diatoms as responsible for the majority of  $NO_3^-$  uptake in the nitracline (Fawcett et al., 2011).

We sought to isolate the impact of competition for  $NH_4^+$  and thus target the causative relationship between  $NH_4^+$ :DIN and variations in PFT relative abundance. To do so, we repeated the set of experiments described above (All, Phys, Warm and OA) but with an alternative parameterization where diatoms were made to have the same growth limitation on  $NH_4^+$  as other phytoplankton, so that there was zero competitive advantage or disadvantage for  $NH_4^+$  between these groups. This simulation was called “model<sub>compete</sub>” and was equivalent to making the dashed black and green lines in Figure 2 the same under all conditions (see upward arrow in Fig. 2). All other traits remained unchanged. Importantly, this included the competitive advantage of diatoms at high  $NO_3^-$  but also their competitive disadvantage at low  $NO_3^-$ . In other words, when DIN was low, diatoms were equally competitive for  $NH_4^+$ , but still suffered their unique limitations associated with  $NO_3^-$ , light, silicate, phosphate, and iron availability, as well as grazing pressure. Meanwhile, “model<sub>control</sub>” used the default parameterization above.

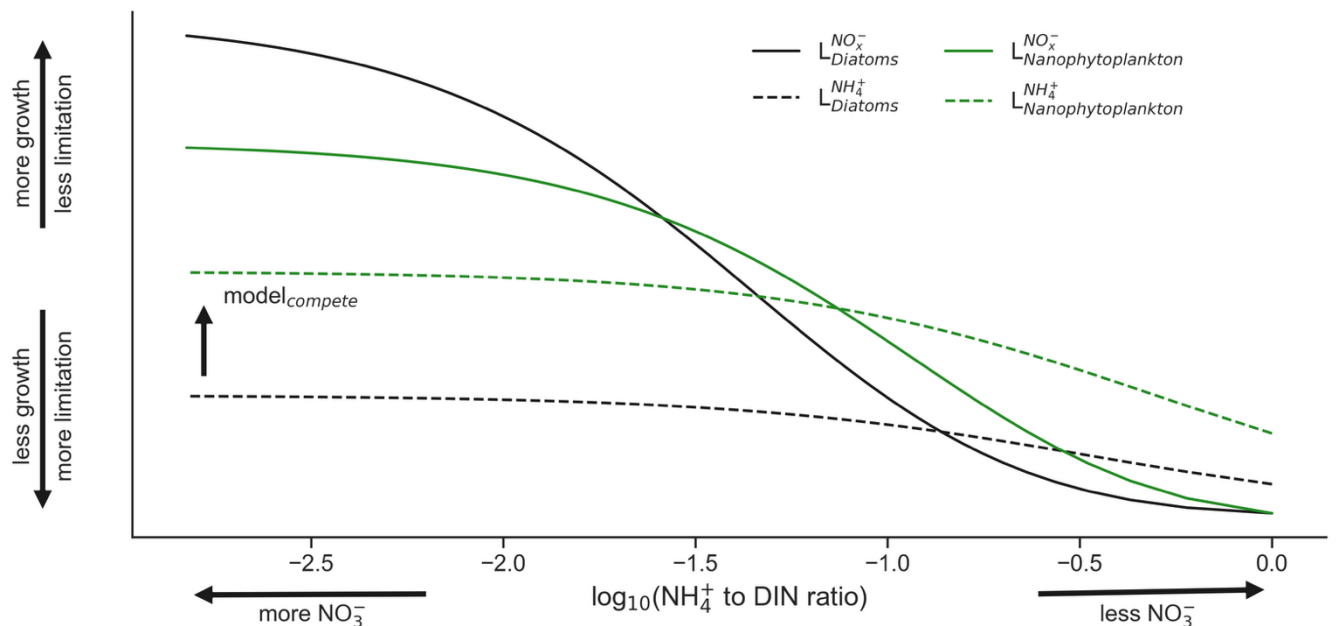


Figure 2. Limitation of the diatom (black) and nanophytoplankton (green) phytoplankton functional types (PFT) in the ocean-biogeochemical model by  $\text{NO}_3^-$  (solid lines) and  $\text{NH}_4^+$  (dashed lines) as a function of the  $\text{NH}_4^+:\text{DIN}$  ratio on a  $\log_{10}$  scale. Note that the nanophytoplankton PFT is always more competitive for  $\text{NH}_4^+$  and is more competitive for  $\text{NO}_3^-$  when  $\text{NO}_3^-$  is low, while diatoms become more competitive for  $\text{NO}_3^-$  when  $\text{NO}_3^-$  is high.”

Line 306: Why surprisingly? Is 70% too high or too low?

Removed.

Line 493: albiet -> albeitt

Corrected.

Line 496: ellaboratiung -> elaborating

Corrected.

Fig. S3: If possible, please add one panel that displays model results from where observations exist.

Included in the figure.

Fig. S8: I believe the unit (or scale) for the right panels is wrong.

We have corrected the figure.